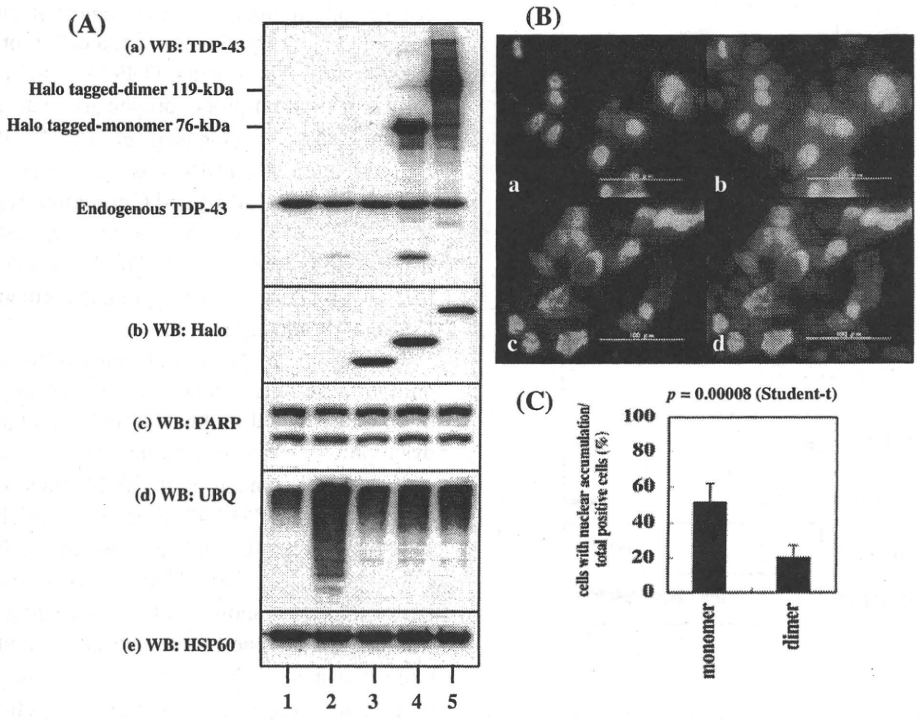

Fig. 7 TDP-43 dimer serves as a seed for promoting aggregation of TDP-43 proteins. **A** The expression of TDP-43 tandem dimer promotes an accumulation of high-molecular-mass TDP-43-immunoreactive proteins. The vectors of Halo-tagged GFP (*lane 3*), TDP-43 FL monomer (*lane 4*), or FL tandem dimer (*lane 5*) were transfected or untransfected (*lanes 1* and *2*) in HEK293 cells with (*lane 2*) or without (*lanes 1, 3–5*) a 24-h treatment of 1-μM MG-132. The protein extract was processed for Western blot with anti-TDP43 antibody (*panel a*), anti-Halo tag antibody (*panel b*), anti-PARP antibody (*panel c*), anti-ubiquitin antibody (*panel d*), or anti-HSP60 antibody, an internal control for protein loading (*panel e*). **B** Cell imaging analysis. HEK293 cells expressing Halo-tagged TDP-43 monomer (*panels a* and *b*) or tandem dimer (*panels c* and *d*) were processed for labeling with Oregon Green (*panels a* and *c*) merged with nuclear labeling with DAPI (*panels b* and *d*). **C** The counting of the number of the cells with nuclear accumulation of Halo-tagged proteins. The average of cell counts of six random fields under the magnification of ×400 is shown with standard deviations

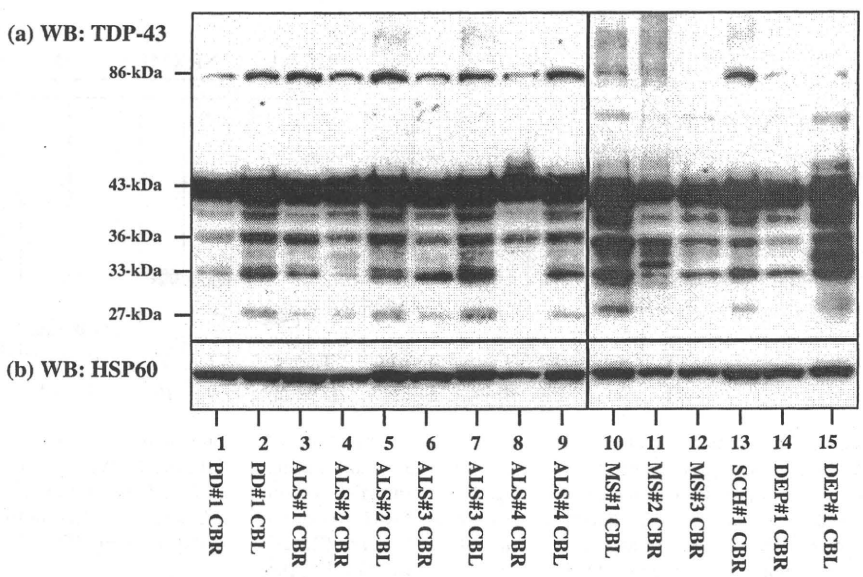

Fig. 8 The constitutive expression of TDP-43 dimer in human brain tissues. The detergent-soluble protein extract of human brain tissues of the cerebrum (*CBR*) (*lanes 1, 3, 4, 6, 8, 11–14*) and the cerebellum (*CBL*) (*lanes 2, 5, 7, 9, 10, 15*), derived from PD#1 (*lanes 1* and *2*), ALS#1 (*lane 3*), ALS#2 (*lanes 4* and *5*), ALS#3 (*lanes 6* and *7*), ALS#4 (*lanes 8* and *9*), MS#1 (*lane 10*), MS#2 (*lane 11*), MS#3 (*lane 12*), SCH#1 (*lane 13*), and DEP#1 (*lanes 14* and *15*) was processed for Western blot with anti-TDP43 antibody (*upper panels*) or anti-HSP60 antibody, an internal control for protein loading (*lower panels*)

transport of TDP-43 could disturb neuronal function by deregulating gene expression. TDP-43 accumulates in the cytoplasm following inhibition of RNA polymerase II by treatment with actinomycin D (Ayala et al. 2008). The C-terminal domain is the most important part for maintenance of solubility and cellular localization of TDP-43, while disruption of the RRM1 domain increases TDP-43 binding to the chromatin and nuclear matrix (Ayala et al. 2008). The TDP-43 mutant protein defective in the nuclear localization signal (NLS) forms cytoplasmic aggregates, while the mutant defective in the nuclear export signal (NES) constitutes nuclear aggregates (Winton et al. 2008). Inhibition of proteasome function by MG-132 enhances the aggregate formation in the NLS-defective mutant (Nonaka et al. 2009b). The overexpression of TDP-43 C-terminal fragment is sufficient to generate hyperphosphorylated and ubiquitinated cytoplasmic aggregates that could alter the exon splicing pattern (Zhang et al. 2009). Although overexpression of the wild-type human TDP-43 protein is toxic to yeast and rat cells (Johnson et al. 2008; Tatom et al. 2009), overexpression of the tandem dimer of TDP-43 did not cause acute cytotoxicity in HEK293 cells in this study.

In this study, the levels of expression of TDP-43 dimer were unaltered in HEK293 cells by treatment with MG-132 or overexpression of ubiqulin-1 (UBQLN1). The ubiqulin family proteins, composed of an N-terminus ubiquitin-like (UBL) domain and a C-terminal ubiquitin-associated (UBA) domain separated by a central Sti1-like repeat, physically interact with both proteasomes and ubiquitin ligases (Ford and Monteiro 2006). UBQLN1, capable of forming a dimer via the central region, promotes the formation of cytoplasmic aggregates of TDP-43, and regulates the proteasome and autophagosome targeting of TDP-43 aggregates (Kim et al. 2008). Polyubiquitinated TDP-43 interacts with the UBA domain of UBQLN1 (Kim et al. 2008). We found that following the expression of the tandem TDP-43 dimer, accumulated high-molecular-mass TDP-43-immunoreactive proteins are unlikely to be ubiquitinated. The 86-kDa TDP-43 dimer constitutively expressed in cultured human cells might not interact with UBQLN1, because it is unlikely to be modified by polyubiquitination.

The present observations suggest that the 86-kDa TDP-43-immunoreactive protein represents a very small amount of dimerized TDP-43 expressed constitutively in normal cells under physiological conditions. We suppose that this dimerized TDP-43 might serve as a starting seed that triggers aggregation of TDP-43 under pathological conditions of TDP-43 proteinopathy. This hypothesis warrants further immunohistochemical and neurochemical investigations, including the establishment of TDP-43-dimer-specific antibodies.

Acknowledgments Human brain tissues were provided by Research Resource Network (RRN), Japan. This work was supported by a research grant to J-IS from the High-Tech Research Center Project, the Ministry of Education, Culture, Sports, Science and Technology (MEXT), Japan (S0801043) and a grant from Research on Intractable Diseases, the Ministry of Health, Labour and Welfare of Japan.

References

Arai T, Hasegawa M, Akiyama H, Ikeda K, Nonaka T, Mori H, Mann D, Tsuchiya K, Yoshida M, Hashizume Y, Oda T (2006) TDP-43 is a component of ubiquitin-positive tau-negative inclusions in frontotemporal lobar degeneration and amyotrophic lateral sclerosis. Biochem Biophys Res Commun 351:602–611

Ayala YM, Pantano S, D'Ambrogio A, Buratti E, Brindisi A, Marchetti C, Romano M, Baralle FE (2005) Human, Drosophila, and *C. elegans* TDP43: nucleic acid binding properties and splicing regulatory function. J Mol Biol 348:575–588

Ayala YM, Zago P, D'Ambrogio A, Xu YF, Petrucelli L, Buratti E, Baralle FE (2008) Structural determinants of the cellular localization and shuttling of TDP-43. J Cell Sci 121:3778–3785

Buratti E, Baralle FE (2008) Multiple roles of TDP-43 in gene expression, splicing regulation, and human disease. Front Biosci 13:867–878

Buratti E, Brindisi A, Giombi M, Tisminetzky S, Ayala YM, Baralle FE (2005) TDP-43 binds heterogeneous nuclear ribonucleoprotein A/B through its C-terminal tail: an important region for the inhibition of cystic fibrosis transmembrane conductance regulator exon 9 splicing. J Biol Chem 280:37572–37584

Choi J, Sullards MC, Olzmann JA, Rees HD, Weintraub ST, Bostwick DE, Gearing M, Levey AI, Chin LS, Li L (2006) Oxidative damage of DJ-1 is linked to sporadic Parkinson and Alzheimer diseases. J Biol Chem 281:10816–10824

Ford DL, Monteiro MJ (2006) Dimerization of ubiquilin is dependent upon the central region of the protein: evidence that the monomer, but not the dimer, is involved in binding presenilins. Biochem J 399:397–404

Geser F, Martinez-Lage M, Kwong LK, Lee VM, Trojanowski JQ (2009) Amyotrophic lateral sclerosis, frontotemporal dementia and beyond: the TDP-43 diseases. J Neurol 256:1205–1214

Hasegawa M, Arai T, Nonaka T, Kametani F, Yoshida M, Hashizume Y, Beach TG, Buratti E, Baralle F, Morita M, Nakano I, Oda T, Tsuchiya K, Akiyama H (2008) Phosphorylated TDP-43 in frontotemporal lobar degeneration and amyotrophic lateral sclerosis. Ann Neurol 64:60–70

Johnson BS, McCaffery JM, Lindquist S, Gitler AD (2008) A yeast TDP-43 proteinopathy model: exploring the molecular determinants of TDP-43 aggregation and cellular toxicity. Proc Natl Acad Sci USA 105:6439–6444

Johnson BS, Snead D, Lee JJ, McCaffery JM, Shorter J, Gitler AD (2009) TDP-43 is intrinsically aggregation-prone and ALS-linked mutations accelerate aggregation and increase toxicity. J Biol Chem 284:20329–20339

Kabashi E, Valdmanis PN, Dion P, Spiegelman D, McConkey BJ, Vande Velde C, Bouchard JP, Lacomblez L, Pochigaeva K, Salachas F, Pradat PF, Camu W, Meininger V, Dupre N, Rouleau GA (2008) TARDBP mutations in individuals with sporadic and familial amyotrophic lateral sclerosis. Nat Genet 40:572–574

Kametani F, Nonaka T, Suzuki T, Arai T, Dohmae N, Akiyama H, Hasegawa M (2009) Identification of casein kinase-1 phosphorylation sites on TDP-43. Biochem Biophys Res Commun 382:405–409

Kim SH, Shi Y, Hanson KA, Williams LM, Sakasai R, Bowler MJ, Tibbetts RS (2008) Potentiation of ALS-associated TDP-43 aggregation by the proteasome-targeting factor, Ubiquilin 1. J Biol Chem 284:8083–8092

Kuo PH, Doudeva LG, Wang YT, Shen CK, Yuan HS (2009) Structural insights into TDP-43 in nucleic-acid binding and domain interactions. Nucleic Acids Res 37:1799–1808

Moisse K, Volkening K, Leystra-Lantz C, Welch I, Hill T, Strong MJ (2009) Divergent patterns of cytosolic TDP-43 and neuronal progranulin expression following axotomy: implications for TDP-43 in the physiological response to neuronal injury. Brain Res 1249:202–211

Neumann M, Sampathu DM, Kwong LK, Truax AC, Micsenyi MC, Chou TT, Bruce J, Schuck T, Grossman M, Clark CM, McCluskey LF, Miller BL, Masliah E, Mackenzie IR, Feldman H, Feiden W, Kretzschmar HA, Trojanowski JQ, Lee VM (2006) Ubiquitinated TDP-43 in frontotemporal lobar degeneration and amyotrophic lateral sclerosis. Science 314:130–133

Neumann M, Kwong LK, Lee EB, Kremmer E, Flatley A, Xu Y, Forman MS, Troost D, Kretzschmar HA, Trojanowski JQ, Lee VM (2009) Phosphorylation of S409/410 of TDP-43 is a consistent feature in all sporadic and familial forms of TDP-43 proteinopathies. Acta Neuropathol 117:137–149

Nonaka T, Kametani F, Arai T, Akiyama H, Hasegawa M (2009a) Truncation and pathogenic mutations facilitate the formation of intracellular aggregates of TDP-43. Hum Mol Genet 18: 3353–3364

Nonaka T, Arai T, Buratti E, Baralle FE, Akiyama H, Hasegawa M (2009b) Phosphorylated and ubiquitinated TDP-43 pathological inclusions in ALS and FTLD-U are recapitulated in SH-SY5Y cells. FEBS Lett 583:394–400

Ou SH, Wu F, Harrich D, García-Martínez LF, Gaynor RB (1995) Cloning and characterization of a novel cellular protein, TDP-43, that binds to human immunodeficiency virus type 1 TAR DNA sequence motifs. J Virol 69:3584–3596

Satoh J, Obayashi S, Misawa T, Sumiyoshi K, Oosumi K, Tabunoki H (2009) Protein microarray analysis identifies human cellular prion protein interactors. Neuropathol Appl Neurobiol 35:16–35

Tatom JB, Wang DB, Dayton RD, Skalli O, Hutton ML, Dickson DW, Klein RL (2009) Mimicking aspects of frontotemporal lobar degeneration and Lou Gehrig's disease in rats via TDP-43 overexpression. Mol Ther 17:607–613

Wang IF, Wu LS, Shen CK (2008) TDP-43: an emerging new player in neurodegenerative diseases. Trends Mol Med 14:479–485

Winton MJ, Igaz LM, Wong MM, Kwong LK, Trojanowski JQ, Lee VM (2008) Disturbance of nuclear and cytoplasmic TAR DNA-binding protein (TDP-43) induces disease-like redistribution, sequestration, and aggregate formation. J Biol Chem 283: 13302–13309

Zhang YJ, Xu YF, Dickey CA, Buratti E, Baralle F, Bailey R, Pickering-Brown S, Dickson D, Petrucelli L (2007) Progranulin mediates caspase-dependent cleavage of TAR DNA binding protein-43. J Neurosci 27:10530–10534

Zhang YJ, Xu YF, Cook C, Gendron TF, Roettges P, Link CD, Lin WL, Tong J, Castanedes-Casey M, Ash P, Gass J, Rangachari V, Buratti E, Baralle F, Golde TE, Dickson DW, Petrucelli L (2009) Aberrant cleavage of TDP-43 enhances aggregation and cellular toxicity. Proc Natl Acad Sci USA 106:7607–7612

Neuropathology and Applied Neurobiology (2010), **36**, 320–330 doi: 10.1111/j.1365-2990.2010.01076.x

Aberrant microRNA expression in the brains of neurodegenerative diseases: miR-29a decreased in Alzheimer disease brains targets neurone navigator 3

M. Shioya*, S. Obayashi*, H. Tabunoki*, K. Arimat, Y. Saito‡, T. Ishida§ and J. Satoh*

**Department of Bioinformatics and Molecular Neuropathology, Meiji Pharmaceutical University, †Department of Psychiatry, National Center Hospital, NCNP, ‡Department of Laboratory Medicine, National Center Hospital, NCNP, Tokyo, and §Department of Pathology and Laboratory Medicine, Kohnodai Hospital, International Medical Center, Chiba, Japan*

M. Shioya, S. Obayashi, H. Tabunoki, K. Arima, Y. Saito, T. Ishida and J. Satoh (2010) *Neuropathology and Applied Neurobiology* 36, 320–330

Aberrant microRNA expression in the brains of neurodegenerative diseases: miR-29a decreased in Alzheimer disease brains targets neurone navigator 3

Aims: MicroRNAs (miRNAs) are small non-coding RNAs that regulate translational repression of target mRNAs. Accumulating evidence indicates that various miRNAs, expressed in a spatially and temporally controlled that manner in the brain plays a key role in neuronal development. However, at present, the pathological implication of aberrant miRNA expression in neurodegenerative events remains largely unknown. To identify miRNAs closely associated with neurodegeneration, we performed miRNA expression profiling of brain tissues of various neurodegenerative diseases. **Methods:** We initially studied the frontal cortex derived from three amyotrophic lateral sclerosis patients by using a microarray of 723 human miRNAs. This was followed by enlargement of study population with quantitative RT-PCR analysis ($n = 21$). **Results:** By microarray analysis, we identified up-regulation of miR-29a, miR-29b and miR-338-3p in amyotrophic lateral sclerosis brains, but due to a great interindividual variation, we could not validate these results by quantitative RT-PCR. However, we found significant down-regulation of miR-29a in Alzheimer disease (AD) brains. The database search on TargetScan, PicTar and miRBase Target identified neurone navigator 3 (NAV3), a regulator of axon guidance, as a principal target of miR-29a, and actually NAV3 mRNA levels were elevated in AD brains. MiR-29a-mediated down-regulation of NAV3 was verified by the luciferase reporter assay. By immunohistochemistry, NAV3 expression was most evidently enhanced in degenerating pyramidal neurones in the cerebral cortex of AD. **Conclusions:** These observations suggest the hypothesis that underexpression of miR-29a affects neurodegenerative processes by enhancing neuronal NAV3 expression in AD brains.

Keywords: Alzheimer disease, bioinformatics, microarray, miR-29a, neurone navigator 3, real-time RT-PCR

Introduction

MicroRNAs (miRNAs) constitute a class of endogenous small non-coding RNAs conserved through the evolution [1]. miRNAs mediate post-transcriptional regulation of protein-coding genes by binding to the 3′ untranslated region (3′UTR) of target mRNAs, leading to translational inhibition or mRNA degradation, depending on the degree of sequence complementarity. The primary miRNAs are transcribed from the intra- and inter-genetic regions of the genome by RNA polymerase II, followed by processing by the RNase III enzyme Drosha into pre-miRNAs. After

Correspondence: Jun-ichi Satoh, Department of Bioinformatics and Molecular Neuropathology, Meiji Pharmaceutical University, 2-522-1 Noshio, Kiyose, Tokyo 204-8588, Japan. Tel: +81 42 4958678; Fax: +81 42 4958678; E-mail: satoj@my-pharm.ac.jp

nuclear export, they are cleaved by the RNase III enzyme Dicer into mature miRNAs consisting of approximately 22 nucleotides. Finally, a single-stranded miRNA is loaded on to the RNA-induced silencing complex, where the seed sequence located at positions 2–8 from the 5′ end of the miRNA plays a pivotal role in binding to the target mRNA. The miRNAs in a whole cell regulate approximately 30% of all protein-coding genes [2]. A single miRNA is capable of reducing the production of hundreds of proteins [3]. Thus, by targeting multiple transcripts and affecting expression of numerous proteins, miRNAs play a key role in cellular development, differentiation, proliferation, apoptosis and metabolism.

Increasing evidence indicated that various miRNAs, expressed in a spatially and temporally controlled manner in the brain, are involved in neuronal development, differentiation and synaptic plasticity [4]. miR-134 localized to the synaptodendritic compartment of hippocampal neurones regulates synaptic plasticity by inhibiting translation of Lim-domain-containing protein kinase 1 [5]. miR-30a-5p, a miRNA enriched in layer III pyramidal neurones in the human prefrontal cortex, decreases brain-derived neurotrophic factor protein levels [6]. Because a single miRNA has a great impact on the expression of numerous downstream mRNA targets, deregulation of miRNA function in the brain affects diverse cellular signalling pathways essential for neuronal survival and protection against neurodegeneration [7].

The transcription factor Pitx3 indispensable for differentiation of dopaminergic neurones transcribes miR-133b, which in turn suppresses Pitx3 expression [8]. The levels of expression of miR-133b are substantially reduced in dopaminergic neurones in Parkinson disease (PD) brains [8]. The expression of miR-107 that inhibits the production of the β-site amyloid precursor protein cleaving enzyme 1 (BACE1) is reduced in the cerebral cortex of the patients with Alzheimer disease (AD) in the earliest stage [9]. BACE1 is also a target gene for miR-29, and the expression of miR-29a/b-1 cluster is reduced, inversely correlated with BACE1 protein levels, in the anterior temporal cortex of a subgroup of AD patients [10]. The levels of miR-298 and miR-328, both of which decrease the expression of mouse BACE1 protein, are reduced in the hippocampus of aged APPSwe/PS1 transgenic mice [11]. The expression of miR-106b that targets amyloid precursor protein is decreased in the anterior temporal cortex of AD patients [12]. Up-regulation of the nuclear factor NFκB-responsive miR-146a induces down-regulation of complement factor H, an anti-inflammatory mediator in AD brains [13]. Although approximately 70% of presently identified miRNAs are expressed in the brain, physiological and pathogenetic roles of most of these remain unknown [14].

In the present study, to identify miRNAs aberrantly expressed in the brains of human neurodegenerative diseases, we initially studied miRNA expression profiles of the frontal cortex of three amyotrophic lateral sclerosis (ALS) patients on a miRNA microarray. Following enlargement of the study population, we found significant down-regulation of miR-29a in AD brains, being consistent with the previous observations [10]. We identified neurone navigator 3 (NAV3) as a principal target of miR-29a by bioinformatics database search and luciferase reporter assay. NAV3 expression was most evidently enhanced in degenerating pyramidal neurones in the cerebral cortex of AD. These results suggest that the interaction between miR-29a and NAV3 might play a role in neurodegenerative processes of AD.

Materials and methods

Human brain tissues

All the brain tissues of the frontal cortex were obtained from Research Resource Network, Japan. Written informed consent was obtained at autopsy form all the cases examined. The Ethics Committee of both National Center of Neurology and Psychiatry and International Medical Center of Japan approved the present study. The present study includes seven AD patients composed of four men and three women with the mean age of 69.1 ± 9.2 years, and 14 non-AD patients composed of eight men and six women with the mean age of 73.1 ± 10.1 years. The latter include four patients with PD, six patients with ALS and four subjects who died of non-neurological causes. The neuropsychiatric disease patients were clinically diagnosed as AD, PD or ALS by board-certified neurologists and psychiatrists, and the clinical diagnosis was verified by comprehensive examination of autopsied brains by three certified neuropathologists (KA, YS, TI). All AD cases were satisfied with the Consortium to Establish a Registry for Alzheimer's Disease criteria for diagnosis of definite AD [15], and were categorized into the stage C or B of amyloid deposition and the stage VI or IV of neurofibrillary degeneration, following the Braak staging system [16]. The *post mortem* interval of

the cases ranges from 1.1 to 14 h with the average interval of 5.5 ± 4.1 h before freezing the brain tissues for storage at −80°C. Although a recent study showed limited stability of specific brain-enriched miRNAs [17], we found that the quality of RNA of frozen brain tissues with *post mortem* interval longer than 10 h is still sufficient for microarray analysis (data not shown). The characteristics of the study population are summarized in Table S1 online.

MiRNA expression profiling

Total RNA enriched in miRNA was isolated from frozen brain tissues by using mirVana miRNA isolation kit (Ambion, Austin, TX, USA). We initially studied RNA samples isolated from the frontal cortex of three ALS patients. They were individually processed for miRNA expression profiling on a human miRNA microarray version 2 (Agilent Technologies, Palo Alto, CA, USA). The array includes 723 human miRNAs based on the miRBase release 10.1 (http://microrna.sanger.ac.uk). The human frontal cortex total RNA of a 79-year-old Caucasian man who died of bladder cancer (AM6810, Ambion) was utilized as a universal reference. The quality of RNA was validated by identification of 18S rRNA and 28S rRNA peaks on Agilent 2100 Bioanalyzer with a RNA 6000 nano kit (Agilent Technologies). Microarray analysis was performed according to the manufacturer's instruction. In brief, 100 nanogram of total RNA was dephosphorylated by calf intestine alkaline phosphatase (Takara Bio, Shiga, Japan). Three prime end of dephosphorylated RNA was labelled with Cyanine 3-cytidine bisphosphate by T4 RNA ligase. The microarray was hybridized with labelled RNA at 55°C for 20 h, washed, and processed for scanning on an Agilent microarray scanner. The signal intensity was quantified by using Feature Extraction Software version 9.9.3.1 (Agilent Technologies).

Quantitative real-time RT-PCR

To quantify miRNA expression levels, TaqMan microRNA assay-based quantitative RT-PCR (qRT-PCR) was performed on the 7500 Fast Real-Time PCR system (Applied Biosystems, Foster City, CA, USA), following the Delta-Delta Ct method. RNU6B was utilized for an endogenous reference to standardize miRNA expression levels. All the data were calibrated by the universal reference data.

DNase-treated total RNA was processed for cDNA synthesis using oligo$(dT)_{20}$ primers and SuperScript II reverse transcriptase (Invitrogen, Carlsbad, CA, USA). To quantify mRNA expression levels, cDNA was amplified by qRT-PCR on the LightCycler ST300 (Roche Diagnostics, Tokyo, Japan) using SYBR Green I and the NAV3 primer sets consisting of 5′tgacccagagttgtggtctccaag3′ and 5′gtccagtttg gctatcccatgtgc3′. The expression levels of target genes were standardized against those of the glyceraldehyde-3-phosphate dehydrogenase gene detected in identical cDNA samples. All the assays were performed in triplicate.

MiRNA target prediction

The target mRNAs that have the potential binding sites for individual miRNAs were identified by searching them on public databases endowed with prediction algorithms, such as TargetScan (http://targetscan.org), PicTar (http://pictar.mdc-berlin.de) and miRBase Target (http://www.mirbase.org) [18].

Reporter assay

The precursor of hsa-miR-29a (GeneBank Accession No. AF017104) was amplified by PCR with PfuTurbo DNA polymerase (Stratagene, La Jolla, CA, USA) and a set of sense and antisense primers composed of 5′cgggatc ccgctggatttagtaagatttgggccct3′ and 5′cccaagcttgggaacg gtcaccaatacatttcctc3′. Then, it was cloned in the expression vector pBApo-CMV-Neo (Takara Bio) at the BamHI/HindIII cloning site. The 3′UTR sequence of the human NAV3 gene spanning the nucleotide position 379727-380353 that surrounds a conserved miR-29a target sequence 5′aggaacatttcctatggtgctg3′ (GenBank Accession No. NC_000012) was amplified by PCR with a set of sense and antisense primers composed of 5′ctaggcgatcgcaca aatccaagaggccagtcctc3′ and 5′ctaggtttaaacctctttcactta gaactggatgg3′. Then, it was cloned in the dual luciferase reporter vector psiCHECK2 (Promega, Madison, WI, USA) at the SgfI/PmeI cloning site. In this construct, a 6-bp deletion was introduced in the miR-29a seed sequence 5′atggtgctg3′ of the NAV3 3′UTR by using QuikChange II XL site-directed mutagenesis kit (Stratagene). The psiCHECK2 vector contains the *Renilla* luciferase gene to monitor expression changes of the target gene in addition to the firefly luciferase gene controlled by a HSV-TK promoter to normalize the transfection efficacy. At 24 h after cotransfection of the miR-29a expression vector and the

luciferase reporter vector in HEK293 cells, cell lysate was processed for dual luciferase assay on a 20/20 Luminometer (Promega). All the assays were performed in triplicate.

Western blot analysis

To prepare total protein extract, frozen brain tissues were homogenized in RIPA lysis buffer composed of a cocktail of protease inhibitors (Sigma, St. Louis, MO, USA), followed by centrifugation at 13 400 g for 5 min at room temperature (RT). The supernatant was collected for separation on a 12% SDS-PAGE gel. The protein concentration was determined by a Bradford assay kit (Bio-Rad, Hercules, CA, USA). After gel electrophoresis, the protein was transferred onto nitrocellulose membranes, which were immunolabelled at RT overnight with rabbit anti-NAV3 antibody (ab69868; Abcam Japan, Tokyo, Japan). We validated the specificity of the ab69868 antibody by Western blot of a truncated NAV3 protein spanning amino acid residues 1366–1688 (data not shown). The membranes were incubated at RT for 30 min with horseradish peroxidase-conjugated anti-rabbit or goat IgG (Santa Cruz Biotechnology). The specific reaction was visualized by using a chemiluminescent substrate (Pierce, Rockford, IL, USA). After the antibodies were stripped by incubating the membranes at 50°C for 30 min in stripping buffer composed of 62.5 mM Tris-HCl, pH 6.7, 2% SDS and 100 mM 2-mercaptoethanol, they were processed for relabeling with rabbit antibody against 14-3-3 protein (sc-629; Santa Cruz Biotechnology), an internal control for protein loading.

Immunohistochemistry

After deparaffination, tissue sections were heated in 10 mM citrate sodium buffer, pH 6.0 by autoclave at 125°C for 30 s in a temperature-controlled pressure chamber (Dako, Tokyo, Japan). They were exposed to 3% hydrogen peroxide-containing methanol at RT for 15 min to block the endogenous peroxidase activity. The tissue sections were then incubated with phosphate-buffered saline containing 10% normal goat serum at RT for 15 min to block non-specific staining. The tissue sections were incubated in a moist chamber at 4°C overnight with rabbit anti-NAV3 antibody (ab69868). After washing with phosphate-buffered saline, they were labelled at RT for 30 min with a horseradish peroxidase-conjugated secondary antibody (Nichirei, Tokyo, Japan), followed by incubation with a colorizing solution containing diaminobenzidine tetrahydrochloride. For double immunolabelling, after inactivating all the antibodies by autoclaving the sections in the citrate sodium buffer, the tissue sections were incubated with mouse anti-amyloid-beta (Aβ) 11–28 peptide antibody (12B2; Immuno-Biological Laboratories, Gunma, Japan) or rabbit anti-tau antibody (paired 356; AnaSpec, San Jose, CA, USA) at 4°C overnight, followed by incubation with alkaline phosphatase-conjugated secondary antibody (Nichirei), and colorized with New Fuchsin substrate. All the sections were exposed to a counterstain with haematoxylin. For negative controls, the step of incubation with primary antibodies was omitted.

Results

The expression of miR-29a is reduced in the frontal cortex of AD

To identify miRNAs aberrantly expressed in the brains of human neurodegenerative diseases, we initially conducted miRNA expression profiling of frozen brain tissues derived from the frontal cortex of three ALS patients on a microarray. All microarray data are shown in Table S2 online. They were filtered through the following stringent criteria, i.e. the detection of all signals above the threshold, the reference signal value exceeding 100, and the fold change expressed as the signal of ALS divided by the signal of the universal reference greater than 5. After filtration, we identified only three miRNAs, including miR-29a, miR-29b and miR-338-3p, as a group of miRNAs whose expression is substantially up-regulated in all three ALS brains (Table 1). Importantly, rodent cortical neurones express both miR-29a and miR-338-3p [19]. Because miR-29a and miR-29b are located on the identical MIRN29B/MIRN29A gene cluster on chromosome 7q32.3, their putative biological functions are similar [10]. Thereafter, we focused our attention solely on miR-29a and miR-338-3p.

Next, we increased the number of the cases to validate microarray data by qRT-PCR. They include four non-neurological controls (NC), six patients with ALS, seven with AD and four with PD. All qPCR data of individual subjects are shown in Table S3 online. Although we observed a trend for up-regulation in the levels of miR-29a expression in ALS *vs.* NC, the difference did not reach

Table 1. Three microRNAs up-regulated in ALS brains identified by microarray analysis

MicroRNA name	*Accession no.*	*Mature miR sequence*	*Chromosome location*	*Genome context*	*Fold change in ALS-case 1*	*Fold change in ALS-case 2*	*Fold change in ALS-case 4*
hsa-miR-29a	MIMAT0000086	UAGCACCAUCUGAAAUCGGUUA	7q32.3	AC016831.7; intron 2	7.5	11.7	6.3
hsa-miR-29b	MIMAT0000100	UAGCACCAUUUGAAAUCAGUGUU	7q32.3	AC016831.7; intron 2	26.5	41.3	24.2
hsa-miR-338-3p	MIMAT0000763	UCCAGCAUCAGUGAUUUUGUUG	17q25.3	AATK; intron 6, intron 7	15.3	16.0	12.7

RNA samples isolated from frozen frontal cortex tissues of three ALS patients (cases 1, 2 and 4) and a universal reference were processed for miRNA expression profiling on a microarray. The fold change is expressed as the signal of ALS divided by the signal of the universal reference.
ALS, amyotrophic lateral sclerosis.

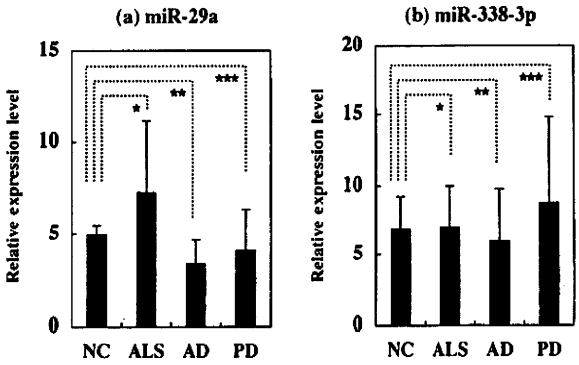

Figure 1. MiR-29a and miR-338-3p expression levels in the brains of neurodegenerative diseases. The expression of microRNA was studied in frozen frontal cortex tissues of non-neurological controls (NC) ($n = 4$), amyotrophic lateral sclerosis (ALS, $n = 6$), Parkinson disease (PD, $n = 4$) and Alzheimer disease (AD, $n = 7$) by TaqMan microRNA assay-based quantitative RT-PCR following the Delta-Delta Ct method. RNU6B was utilized for an endogenous reference to standardize microRNA expression levels. The results were expressed as relative expression levels after calibration with the universal reference data. The panels (**a**,**b**) represent (**a**) miR-29a and (**b**) miR-338-3p. The *P*-value by Student's *t*-test indicates (**a**) ★ 0.263, ★★ 0.041, ★★★ 0.470 and (**b**) ★ 0.956, ★★ 0.676, ★★★ 0.578.

the statistical significance ($P = 0.263$), due to a great interindividual variation (Figure 1**a**). Nevertheless, we found that miR-29a expression levels were significantly reduced in AD ($P = 0.041$), when compared with NC, while the levels of miR-29a expression were not substantially decreased in PD ($P = 0.470$) (Figure 1**a**). On the other hand, the levels of miR-338-3p expression were varied among the cases, and not significantly different among ALS ($P = 0.956$), AD ($P = 0.676$) and PD ($P = 0.578$), when compared with NC (Figure 1**b**).

Database search suggests NAV3 as one of miR-29a targets

Next, we explored putative miR-29a target genes by searching them on three distinct web-accessible miRNA target databases, including TargetScan, PicTar and miRBase Target [18], all of which did not always suggest an identical list of target genes. They identified numerous candidates, which are arranged in order of the highest probability. When top 200 most reliable miR-29a targets identified by each programme were compared, we found 11 genes shared among the three programmes (Table 2). They include fibrillin 1, NAV3, collagen, type V, alpha 3, collagen, type XI, alpha 1, collagen, type I, alpha 2,

Table 2. Predicted miR-29a target genes identified by TargetScan, PicTar and miRBase Target database search

Gene ID	*Gene symbol*	*Gene name*	*TargetScan context score*	*PicTar score*	*miRbase Target p-value*
2200	FBN1	Fibrillin 1	−0.74	8.2288	5.99E-06
89795	NAV3	Neurone navigator 3	−0.68	9.1594	1.15E-04
50509	COL5A3	Collagen, type V, alpha 3	−0.67	12.5665	1.20E-06
1301	COL11A1	Collagen, type XI, alpha 1	−0.65	10.916	5.12E-06
1278	COL1A2	Collagen, type I, alpha 2	−0.63	10.8218	2.80E-04
4678	NASP	Nuclear autoantigenic sperm protein	−0.62	9.5118	1.88E-04
4591	TRIM37	Tripartite motif-containing 37	−0.44	5.6973	2.50E-05
27315	PGAP2	Post-GPI attachment to proteins 2	−0.42	6.0952	1.28E-05
1293	COL6A3	Collagen, type VI, alpha 3	−0.4	6.9128	2.47E-07
29851	ICOS	Inducible T cell co-stimulator	−0.38	7.9789	9.64E-05
116931	MED12L	Mediator complex subunit 12-like	−0.34	9.9157	1.16E-04

MiR-29a target genes were searched on TargetScan, PicTar and miRBase Target databases. The common genes listed within top 200 by each programme are shown following the significance of TargetScan context score.

nuclear autoantigenic sperm protein, tripartite motif-containing 37, post-GPI attachment to proteins 2, collagen, type VI, alpha 3, inducible T cell co-stimulator and mediator complex subunit 12-like. Thus, the genes encoding extracellular matrix components are enriched in the list of miR-29a targets. Among them, we focused our attention on NAV3 for further investigations, because NAV3, alternatively named pore membrane and/or filament interacting like protein 1, is predominantly expressed in the nervous system [20].

MiR-29a directly down-regulates NAV3 expression

The TargetScan search indicated that the 3′UTR of the human NAV3 gene contains two separate miR-29a-binding seed sequences that are conserved through evolution. They are located in the nucleotide position 807–813 with TargetScan context score −0.24 and the position 1831–1837 with TargetScan context score −0.33. We cloned the former with the higher score in the luciferase reporter vector. Then, it was cotransfected with a miR-29a expression vector in HEK293 cells. Overexpression of miR-29a significantly suppressed the expression of the luciferase reporter containing the wild-type target sequence with a % reduction = 24.4 ($P = 0.014$; Figure 2, left panels). In contrast, miR-29a did not affect the expression of the vector containing a 6-bp deletion in the seed sequence ($P = 0.138$; Figure 2, right panels).

The levels of NAV3 mRNA but not of protein are elevated in AD brains

By qRT-PCR analysis, we found that the levels of NAV3 mRNA expression in the frontal cortex were much higher in AD patients, compared with NC subjects, PD patients and ALS patients (Figure 3). By Western blot analysis, the levels of expression of NAV3 protein, composed of two major bands of 100 kDa and 46 kDa, were varied among the cases and not elevated in AD brains, while the levels of 14-3-3 protein, an internal control for protein loading, were almost constant (Figure 4**a,b**, lanes 1–21). There did not exist a clear correlation between NAV3 mRNA and protein levels in each case.

Pyramidal neurones express intense NAV3 immunoreactivity in the frontal cortex of AD brains

Finally, by immunohistochemistry, we investigated the expression of NAV3 in the frontal cortex of AD, ALS or PD. In all the brains examined, large- and medium-sized pyramidal neurones in layers III and V of the cerebral cortex expressed strong NAV3 immunoreactivity located chiefly in the cytoplasm, axons and dendrites (Figure 5**a–d**). Notably, NAV3 immunolabelling was the most intense in neurones presenting with degenerating morphology bearing pyknotic nuclei in AD brains (Figure 5**a,b,f**). A population of non-pyramidal neurones also expressed much weaker NAV3 immunoreactivity, while the great majority of reactive astrocytes, microglia and

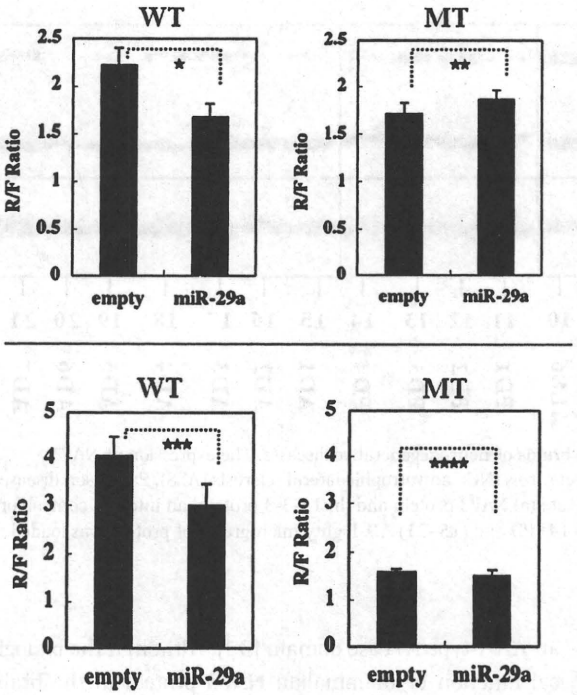

Figure 2. Dual luciferase assay of miR-29a-mediated down-regulation of neurone navigator 3 (NAV3). The precursor of hsa-miR-29a sequence was cloned in the expression vector pBApo-CMV-Neo, while the 3′ untranslated region (3′UTR) sequence of the human NAV3 was cloned in the dual luciferase reporter vector psiCHECK2 that contains the *Renilla* (R) luciferase gene to monitor expression changes of NAV3 in addition to the firefly (F) luciferase gene to normalize the transfection efficacy. A 6-bp deletion was introduced in the miR-29a seed sequence 5′ATGGTGCTG3′ of the NAV3 3′UTR. At 24 h after cotransfection of the miR-29a expression vector or the empty pBApo-CMV-Neo vector with the luciferase reporter vector in HEK293 cells, cell lysate was processed for dual luciferase assay. Two series of the experiments were performed. Each set represents the reporter vector containing (the left) the wild-type (WT) NAV3 3′UTR or (the right) the 6-bp deletion mutant (MT) NAV3 3′UTR. The R/F signal ratio is shown. The *P*-value by Student's *t*-test indicates ★ 0.014, ★★ 0.138, ★★★ 0.037 and ★★★★ 0.289.

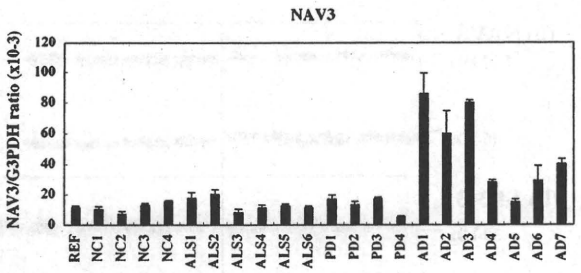

Figure 3. Neurone navigator 3 (NAV3) mRNA expression levels in the brains of neurodegenerative diseases. The expression of NAV3 mRNA was studied in frozen frontal cortex tissues of non-neurological controls (NC, $n = 4$), amyotrophic lateral sclerosis (ALS, $n = 6$), Parkinson disease (PD, $n = 4$) and Alzheimer disease (AD, $n = 7$) by quantitative RT-PCR. The levels of NAV3 mRNA are standardized against those of glyceraldehyde-3-phosphate dehydrogenase (G3PDH) mRNA detected in identical cDNA samples. REF indicates a universal reference derived from the human frontal cortex total RNA (AM6810, Ambion).

oligodendrocytes are devoid of NAV3. In AD brains, a substantial population (<20%) of pyramidal neurones containing tau-immunolabelled neurofibrillary tangles coexpressed intense NAV3 immunoreactivity (Figure 5e). In contrast, Aβ plaques did not typically express NAV3 immunoreactivity in AD brains (Figure 5f).

Discussion

To identify miRNAs aberrantly regulated in the brains of human neurodegenerative diseases, we initially studied miRNA expression profiles of frozen frontal cortex tissues of three ALS patients by using a miRNA microarray. We identified up-regulation of miR-29a, miR-29b and miR-338-3p in ALS brains. Among them, miR-338 is a biomarker candidate for neurodegeneration, because it acts as a negative regulator of neuronal differentiation by suppressing apoptosis-associated tyrosine kinase and cytochrome oxidase complex IV [21,22]. However, following enlargement of the study population by qRT-PCR, we could not verify up-regulation of miR-338-3p in ALS brains. On the other hand, we identified significant down-regulation of miR-29a in AD brains, being consistent with previous observations that miR-29 expression levels are reduced in the anterior temporal cortex of AD patients, associated with substantial elevation of BACE1 protein levels [10]. However, in the present study, the search on three distinct miRNA target databases, such as TargetScan, PicTar and miRBase Target operating on different algorithms, did not identify BACE1 within the top 200 miR-29a targets. These programmes commonly identified NAV3 as one of top-ranking miR-29a targets. We verified the miR-29a-mediated suppression of NAV3 by luciferase reporter assay.

Previous studies showed that miR-29 is involved in translational repression of a wide range of target genes. Down-regulation of miR-29 in the area surrounding the myocardial infarct core enhances fibrosis by de-repressing the expression of a battery of collagen genes [23]. miR-29a represses translation of osteonectin, the most abundant non-collagenous matrix protein in the bone [24]. In

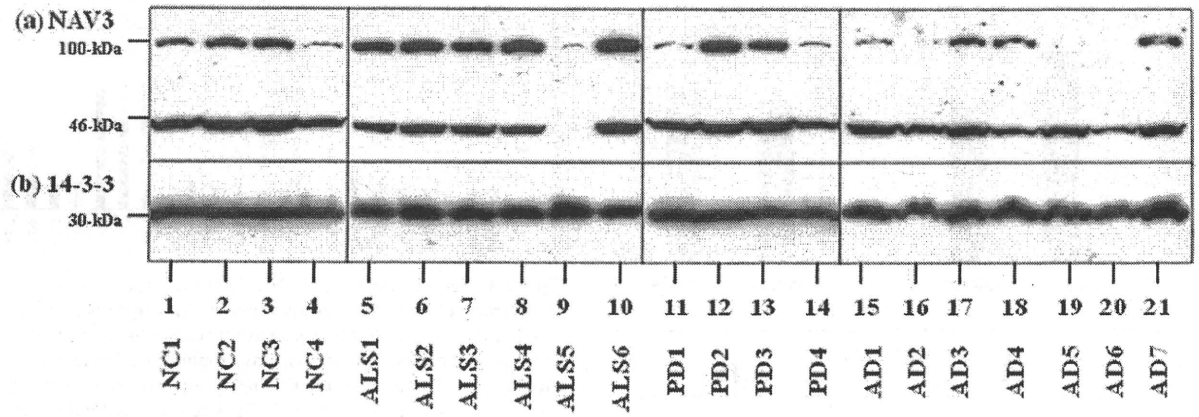

Figure 4. Neurone navigator 3 (NAV3) protein expression levels in the brains of neurodegenerative diseases. The expression of NAV3 protein was studied in frozen frontal cortex tissues of non-neurological controls (NC), amyotrophic lateral sclerosis (ALS), Parkinson disease (PD) and Alzheimer disease (AD) by Western blot. The panels (**a, b**) indicate (a) NAV3 protein and (**b**) 14-3-3 protein, an internal control for protein loading. The lanes (1–21) represent (1–4) NC, (5–10) ALS, (11–14) PD and (15–21) AD. Eighty micrograms of protein was loaded in each lane.

line with these, we identified a panel of extracellular matrix components, such as fibrillin 1, collagen, type V, alpha 3, collagen, type XI, alpha 1 and collagen, type I, alpha 2, as a group of top-ranking miR-29a target genes. The levels of expression of the miR-29 family are reduced in lung cancer, cholangiocarcinoma, chronic lymphocytic leukemia and neuroblastoma, suggesting that miR-29 acts as a proapoptotic anti-oncomir [25–27]. The oncogenic transcription factor cMyc reduces the expression of miR-29 in cancer cells by binding directly to the miR-29 promoter region [28]. By suppressing the expression of PI3 kinase p85α and CDC42, miR-29 activates p53 and induces apoptosis in HeLa cells [29]. miR-29 acts as an enhancer of myogenic differentiation and a suppressor of rhabdomyosarcoma by targeting YY1 transcription factor [30]. miR-29a promotes the epithelial-to-mesenchymal transition of breast cancer cells by suppressing the expression of tristetraprolin [31]. All of these observations suggest that miR-29a modulates cellular differentiation and survival by regulating a wide range of target mRNAs.

Neurone navigator 3 is a member of the neurone navigator protein family expressed predominantly in the central and peripheral nervous systems [20]. In adult mouse brain, NAV3 is expressed chiefly in nuclear membranes of neurones in the cerebral cortex, midbrain, cerebellum and the hippocampal formation [20]. The NAV3 protein structure is characterized by an N-terminal calponin homology domain, several coiled-coil regions, an actin-binding domain, a GTP/ATP-binding domain and an AAA-type ATPase domain [32]. Although the biological function of mammalian NAV3 protein in the brain remains totally unknown, a *Caenorhabditis elegans* gene named unc-53 highly homologous to NAV3, plays a key role in axon guidance [33]. Importantly, NAV2, a paralog of NAV3, plays a central role in neurite outgrowth and axonal elongation in human neuroblastoma cells [34]. Furthermore, the NAV3 gene is occasionally disrupted in primary cutaneous T cell lymphomas by chromosomal translocation, suggesting that NAV3 acts as a tumour suppressor gene [35].

We found that the levels of NAV3 mRNA were elevated in AD brains, although we did not find a correlation between NAV3 mRNA levels by real-time RT-PCR and protein levels by Western blot. The lack of the correlation between mRNA levels and protein abundance might be in part attributable to the differential stability and turnover of mRNA and protein via various post-transcriptional mechanisms, including the selective degradation of proteins by proteasome and autophagosome machineries [36]. Nevertheless, we found that pyramidal neurones in the cerebral cortex expressed strong NAV3 immunoreactivity in both AD and non-AD brains. Furthermore, a substantial population of cortical pyramidal neurones coexpressed NAV3 and neurofibrillary tangles in AD brains, where NAV3 immunoreactivity was the most intense in neurones with degenerating morphology bearing pyknotic nuclei. A previous study performed on mouse brains showed that NAV3 immunoreactivity is

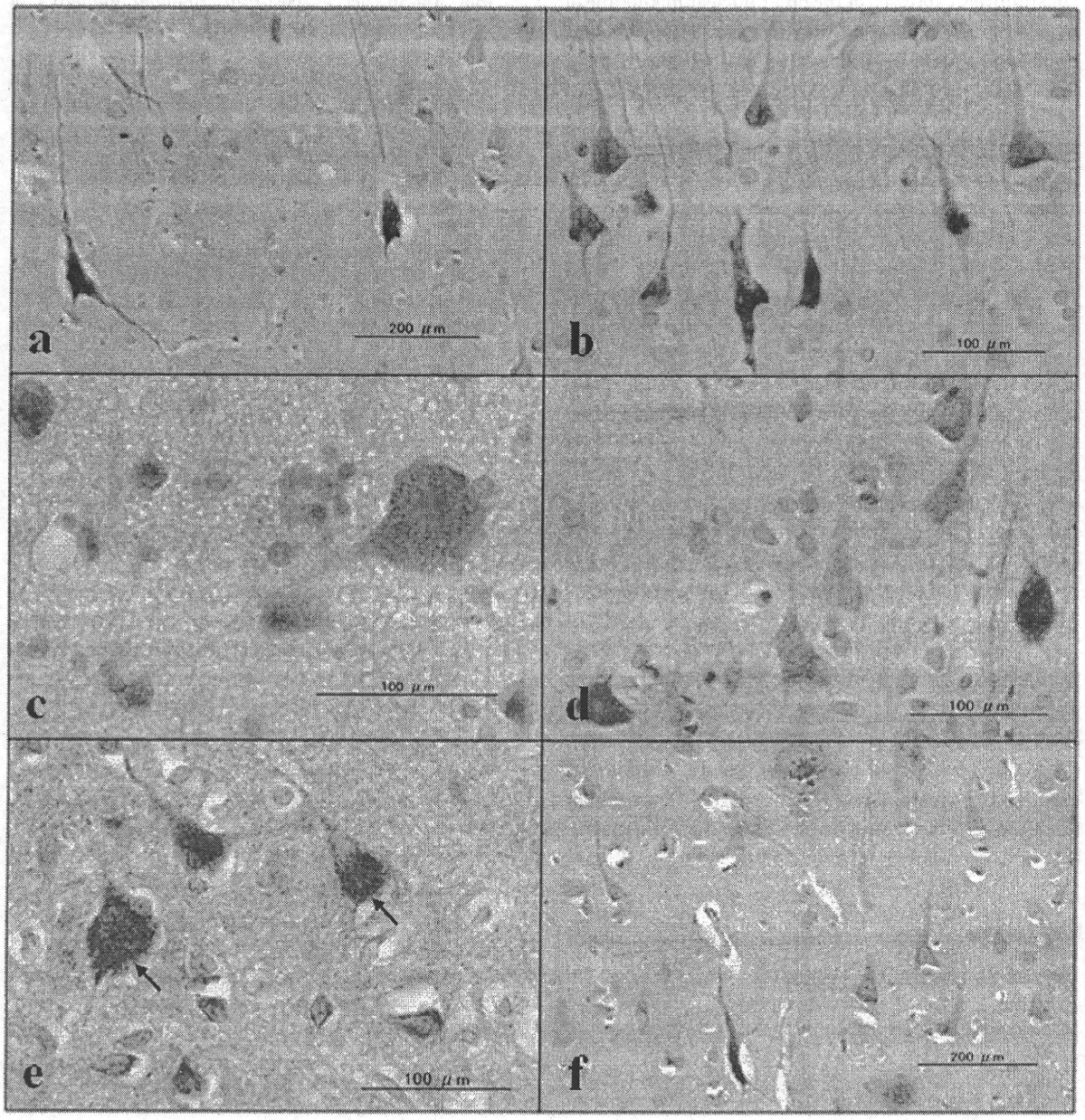

Figure 5. Neurone navigator 3 (NAV3) immunohistochemistry of the brains of neurodegenerative diseases. The expression of NAV3, paired helical filament (PHF)-tau and Aβ was studied in the frontal cortex tissue sections of Alzheimer disease (AD), amyotrophic lateral sclerosis (ALS) and Parkinson disease (PD) by immunohistochemistry. The panels (**a–f**) represent (**a**) NAV3 in AD-case 3, (**b**) NAV3 in AD-case 1, (**c**) NAV3 in ALS-case 4, (**d**) NAV3 in PD-case 3, (**e**) NAV3 (brown) and PHF-tau (red) double immunolabelling of AD-case 1 where the coexpression is indicated by arrows, and (**f**) NAV3 (brown) and Aβ (red) double immunolabelling of AD-case 3. In all the cases, large- and medium-sized pyramidal neurones in layers III and V express strong NAV3 immunoreactivity located in the cytoplasm, axons and dendrites. Notably, NAV3 immunoreactivity is the most intense in neurones with degenerating morphology bearing pyknotic nuclei in AD brains as shown in panels (**a, b, f**).

constitutively expressed at the outer nuclear membrane of neurones, and it is induced in reactive astrocytes after brain injury [20]. In contrast, we did not detect NAV3 immunoreactivity in reactive astrocytes in the brains of AD, PD and ALS. At present, it remains unknown whether enhanced expression of NAV3 in a subpopulation of cortical pyramidal neurones in AD brains reflects some pathogenetic changes or it is attributable to a compensatory mechanism against neurodegenerative events. By miRNA target database search, we found that not only miR-29, but also miR-19, miR-34 and miR-449, potentially down-regulate NAV3 expression (unpublished data), suggesting that multiple miRNAs converge on the regulation of NAV3 expression. Overall, the results of the present study could propose a possible scenario that underexpression of miR-29a affects neurodegenerative processes by up-regulating NAV3 and other miR-29a targets in AD brains. Further studies using large cohorts are required to clarify an active involvement of the miR-29a and NAV3 circuit in progression of neurodegeneration in AD.

Acknowledgements

Human brain tissues were provided by Research Resource Network, Japan. This work was supported by a research grant to J-IS from the High-Tech Research Center Project, the Ministry of Education, Culture, Sports, Science and Technology, Japan (S0801043) and a grant from Research on Intractable Diseases, the Ministry of Health, Labour and Welfare of Japan.

References

1 Kosik KS. The neuronal microRNA system. *Nat Rev Neurosci* 2006; **7**: 911–20
2 Filipowicz W, Bhattacharyya SN, Sonenberg N. Mechanisms of post-transcriptional regulation by microRNAs: are the answers in sight? *Nat Rev Genet* 2008; **9**: 102–14
3 Selbach M, Schwanhäusser B, Thierfelder N, Fang Z, Khanin R, Rajewsky N. Widespread changes in protein synthesis induced by microRNAs. *Nature* 2008; **455**: 58–63
4 Fineberg SK, Kosik KS, Davidson BL. MicroRNAs potentiate neural development. *Neuron* 2009; **64**: 303–9
5 Schratt GM, Tuebing F, Nigh EA, Kane CG, Sabatini ME, Kiebler M, Greenberg ME. A brain-specific microRNA regulates dendritic spine development. *Nature* 2006; **439**: 283–9
6 Mellios N, Huang HS, Grigorenko A, Rogaev E, Akbarian S. A set of differentially expressed miRNAs, including miR-30a-5p, act as post-transcriptional inhibitors of BDNF in prefrontal cortex. *Hum Mol Genet* 2008; **17**: 3030–42
7 Nelson PT, Wang WX, Rajeev BW. MicroRNAs (miRNAs) in neurodegenerative diseases. *Brain Pathol* 2008; **18**: 130–8
8 Kim J, Inoue K, Ishii J, Vanti WB, Voronov SV, Murchison E, Hannon G, Abeliovich A. A MicroRNA feedback circuit in midbrain dopamine neurons. *Science* 2007; **317**: 1220–4
9 Wang WX, Rajeev BW, Stromberg AJ, Ren N, Tang G, Huang Q, Rigoutsos I, Nelson PT. The expression of microRNA miR-107 decreases early in Alzheimer's disease and may accelerate disease progression through regulation of beta-site amyloid precursor protein-cleaving enzyme 1. *J Neurosci* 2008; **28**: 1213–23
10 Hébert SS, Horré K, Nicolaï L, Papadopoulou AS, Mandemakers W, Silahtaroglu AN, Kauppinen S, Delacourte A, De Strooper B. Loss of microRNA cluster miR-29a/b-1 in sporadic Alzheimer's disease correlates with increased BACE1/beta-secretase expression. *Proc Natl Acad Sci USA* 2008; **105**: 6415–20
11 Boissonneault V, Plante I, Rivest S, Provost P. MicroRNA-298 and microRNA-328 regulate expression of mouse β-amyloid precursor protein-converting enzyme 1. *J Biol Chem* 2009; **284**: 1971–81
12 Hébert SS, Horré K, Nicolaï L, Bergmans B, Papadopoulou AS, Delacourte A, De Strooper B. MicroRNA regulation of Alzheimer's amyloid precursor protein expression. *Neurobiol Dis* 2009; **33**: 422–8
13 Lukiw WJ, Zhao Y, Cui JG. An NF-κB-sensitive micro RNA-146a-mediated inflammatory circuit in Alzheimer disease and in stressed human brain cells. *J Biol Chem* 2008; **283**: 31315–22
14 Kocerha J, Kauppinen S, Wahlestedt C. microRNAs in CNS Disorders. *Neuromolecular Med* 2009; **11**: 162–72
15 Mirra SS, Heyman A, McKeel D, Sumi SM, Crain BJ, Brownlee LM, Vogel FS, Hughes JP, van Belle G, Berg L. The Consortium to Establish a Registry for Alzheimer's Disease (CERAD). Part II. Standardization of the neuropathologic assessment of Alzheimer's disease. *Neurology* 1991; **41**: 479–86
16 Braak H, Alafuzoff I, Arzberger T, Kretzschmar H, Del Tredici K. Staging of Alzheimer disease-associated neurofibrillary pathology using paraffin sections and immunocytochemistry. *Acta Neuropathol* 2006; **112**: 389–404
17 Sethi P, Lukiw WJ. Micro-RNA abundance and stability in human brain: specific alterations in Alzheimer's disease temporal lobe neocortex. *Neurosci Lett* 2009; **459**: 100–4
18 Mendes ND, Freitas AT, Sagot MF. Current tools for the identification of miRNA genes and their targets. *Nucleic Acids Res* 2009; **37**: 2419–33
19 Kim J, Krichevsky A, Grad Y, Hayes GD, Kosik KS, Church GM, Ruvkun G. Identification of many microRNAs that

copurify with polyribosomes in mammalian neurons. *Proc Natl Acad Sci USA* 2004; **101**: 360–5
20 Coy JF, Wiemann S, Bechmann I, Bächner D, Nitsch R, Kretz O, Christiansen H, Poustka A. Pore membrane and/or filament interacting like protein 1 (POMFIL1) is predominantly expressed in the nervous system and encodes different protein isoforms. *Gene* 2002; **290**: 73–94
21 Aschrafi A, Schwechter AD, Mameza MG, Natera-Naranjo O, Gioio AE, Kaplan BB. MicroRNA-338 regulates local cytochrome c oxidase IV mRNA levels and oxidative phosphorylation in the axons of sympathetic neurons. *J Neurosci* 2008; **28**: 12581–90
22 Barik S. An intronic microRNA silences genes that are functionally antagonistic to its host gene. *Nucleic Acids Res* 2008; **36**: 5232–41
23 van Rooij E, Sutherland LB, Thatcher JE, DiMaio JM, Naseem RH, Marshall WS, Hill JA, Olson EN. Dysregulation of microRNAs after myocardial infarction reveals a role of miR-29 in cardiac fibrosis. *Proc Natl Acad Sci USA* 2008; **105**: 13027–32
24 Kapinas K, Kessler CB, Delany AM. miR-29 suppression of osteonectin in osteoblasts: regulation during differentiation and by canonical Wnt signaling. *J Cell Biochem* 2009; **108**: 216–24
25 Fabbri M, Garzon R, Cimmino A, Liu Z, Zanesi N, Callegari E, Liu S, Alder H, Costinean S, Fernandez-Cymering C, Volinia S, Guler G, Morrison CD, Chan KK, Marcucci G, Calin GA, Huebner K, Croce CM. MicroRNA-29 family reverts aberrant methylation in lung cancer by targeting DNA methyltransferases 3A and 3B. *Proc Natl Acad Sci USA* 2007; **104**: 15805–10
26 Mott JL, Kobayashi S, Bronk SF, Gores GJ. mir-29 regulates Mcl-1 protein expression and apoptosis. *Oncogene* 2007; **26**: 6133–40
27 Xu H, Cheung IY, Guo HF, Cheung NK. MicroRNA miR-29 modulates expression of immunoinhibitory molecule B7-H3: potential implications for immune based therapy of human solid tumors. *Cancer Res* 2009; **69**: 6275–81
28 Chang TC, Yu D, Lee YS, Wentzel EA, Arking DE, West KM, Dang CV, Thomas-Tikhonenko A, Mendell JT. Widespread microRNA repression by Myc contributes to tumorigenesis. *Nat Genet* 2008; **40**: 43–50
29 Park SY, Lee JH, Ha M, Nam JW, Kim VN. miR-29 miRNAs activate p53 by targeting p85 alpha and CDC42. *Nat Struct Mol Biol* 2009; **16**: 23–9
30 Wang H, Garzon R, Sun H, Ladner KJ, Singh R, Dahlman J, Cheng A, Hall BM, Qualman SJ, Chandler DS, Croce CM, Guttridge DC. NF-kappaB-YY1-miR-29 regulatory circuitry in skeletal myogenesis and rhabdomyosarcoma. *Cancer Cell* 2008; **14**: 369–81
31 Gebeshuber CA, Zatloukal K, Martinez J. miR-29a suppresses tristetraprolin, which is a regulator of epithelial polarity and metastasis. *EMBO Rep* 2009; **10**: 400–5
32 Maes T, Barceló A, Buesa C. Neuron navigator: a human gene family with homology to *unc-53*, a cell guidance gene from *Caenorhabditis elegans*. *Genomics* 2002; **80**: 21–30
33 Hekimi S, Kershaw D. Axonal guidance defects in a *Caenorhabditis elegans* mutant reveal cell-extrinsic determinants of neuronal morphology. *J Neurosci* 1993; **13**: 4254–71
34 Muley PD, McNeill EM, Marzinke MA, Knobel KM, Barr MM, Clagett-Dame M. The atRA-responsive gene neuron navigator 2 functions in neurite outgrowth and axonal elongation. *Dev Neurobiol* 2008; **68**: 1441–53
35 Karenko L, Hahtola S, Päivinen S, Karhu R, Syrjä S, Kähkönen M, Nedoszytko B, Kytölä S, Zhou Y, Blazevic V, Pesonen M, Nevala H, Nupponen N, Sihto H, Krebs I, Poustka A, Roszkiewicz J, Saksela K, Peterson P, Visakorpi T, Ranki A. Primary cutaneous T-cell lymphomas show a deletion or translocation affecting *NAV3*, the human *UNC-53* homologue. *Cancer Res* 2005; **65**: 8101–10
36 Laloo B, Simon D, Veilla V, Lauzel D, Guyonnet-Duperat V, Moreau-Gaudry F, Sagliocco F, Grosset C. Analysis of post-transcriptional regulations by a functional, integrated, and quantitative method. *Mol Cell Proteomics* 2009; **8**: 1777–88

Supporting information

Additional Supporting Information may be found in the online version of this article:

Table S1. Characteristics of the study population.
Table S2. MicroRNA expression profiling of the frontal cortex of three ALS patients on a human miRNA microarray.
Table S3. Real-time RT-PCR analysis of miR-29a expression in the frontal cortex of human neurodegenerative diseases.

Please note: Wiley-Blackwell are not responsible for the content or functionality of any supporting materials supplied by the authors. Any queries (other than missing material) should be directed to the corresponding author for the article.

Received 18 December 2009
Accepted after revision 1 February 2010
Published online Article Accepted on 25 February 2010

Clinical and Experimental Neuroimmunology 1 (2010) 127–140

REVIEW ARTICLE

Bioinformatics approach to identifying molecular biomarkers and networks in multiple sclerosis

Jun-ichi Satoh

Department of Bioinformatics and Molecular Neuropathology, Meiji Pharmaceutical University, Tokyo, Japan

Keywords
bioinformatics; KeyMolnet; molecular network; multiple sclerosis; systems biology

Correspondence
Jun-ichi Satoh MD, PhD, Department of Bioinformatics and Molecular Neuropathology, Meiji Pharmaceutical University,
2-522-1 Noshio, Kiyose, Tokyo 204-8588, Japan.
Tel: +81-42-495-8678
Fax: +81-42-495-8678
Email: satoj@my-pharm.ac.jp

Received: 6 June 2010; accepted: 3 August 2010.

Abstract

Multiple sclerosis (MS) is an inflammatory demyelinating disease of the central nervous system (CNS) white matter mediated by an autoimmune process triggered by a complex interplay between genetic and environmental factors, in which the precise molecular pathogenesis remains to be comprehensively characterized. The global analysis of genome, transcriptome, proteome and metabolome, collectively termed omics, promotes us to characterize the genome-wide molecular basis of MS. However, as omics studies produce high-throughput experimental data at one time, it is often difficult to find out the meaningful biological implications from huge datasets. Recent advances in bioinformatics and systems biology have made major breakthroughs by illustrating the cell-wide map of complex molecular interactions with the aid of the literature-based knowledgebase of molecular pathways. The integration of omics data derived from the disease-affected cells and tissues with underlying molecular networks provides a rational approach not only to identifying the disease-relevant molecular markers and pathways, but also to designing the network-based effective drugs for MS. (Clin. Exp. Neuroimmunol. doi: 10.1111/j.1759-1961.2010.00013.x, September 2010)

Introduction

Multiple sclerosis (MS) is an inflammatory demyelinating disease affecting exclusively the central nervous system (CNS) white matter mediated by an autoimmune process triggered by a complex interplay between genetic and environmental factors.[1] Intravenous administration of interferon-gamma (IFNγ) provoked acute relapses of MS, indicating a pivotal role of proinflammatory T helper type 1 (Th1) lymphocytes. More recent studies proposed the pathogenic role of Th17 lymphocytes in sustained tissue damage in MS.[2] MS shows a great range of phenotypic variability. The disease is classified into relapsing-remitting MS (RRMS), secondary progressive MS (SPMS) or primary progressive MS (PPMS) with respect to the clinical course. Pathologically, MS shows a remarkable heterogeneity in the degree of inflammation, complement activation, antibody deposition, demyelination and remyelination, oligodendrocyte apoptosis, and axonal degeneration.[3] Currently available drugs in clinical practice of MS, including interferon-beta (IFNβ), glatiramer acetate, mitoxantrone, FTY720 and natalizumab, have proven only limited efficacies in subpopulations of the patients.[4] These observations suggest the hypothesis that MS is a kind of neurological syndrome caused by different immunopathological mechanisms leading to the final common pathway that provokes inflammatory demyelination. Therefore, the identification of specific biomarkers relevant to the heterogeneity of MS is highly important to establish the molecular mechanism-based personalized therapy in MS.

After the completion of the Human Genome Project in 2003, the global analysis of genome, transcriptome, proteome and metabolome, collectively termed omics, promotes us to characterize the genome-wide molecular basis of the diseases, and helps us to identify disease-specific molecular signatures

and biomarkers for diagnosis and prediction of prognosis. Actually, the genome-wide association study (GWAS) of MS revealed novel risk alleles for susceptibility of MS.[5] The comprehensive transcriptome and proteome profiling of brain tissues and lymphocytes identified key molecules aberrantly regulated in MS, whose role has not been previously predicted in the pathogenesis of MS.[6,7] Most recently, the application of next-generation sequencing technology to personal genomes has enabled us to investigate the genetic basis of MS at the level of individual patients.[8]

Because omics studies usually produce high-throughput experimental data at one time, it is often difficult to find out the meaningful biological implications from such a huge dataset. Recent advances in bioinformatics and systems biology have made major breakthroughs by showing the cell-wide map of complex molecular interactions with the aid of the literature-based knowledgebase of molecular pathways.[9] The logically arranged molecular networks construct the whole system characterized by robustness, which maintains the proper function of the system in the face of genetic and environmental perturbations.[10] In the scale-free molecular network, targeted disruption of limited numbers of critical components designated the hub, on which the biologically important molecular connections concentrate, could disturb the whole cellular function by destabilizing the network.[11] From the point of these views, the integration of omics data derived from the disease-affected cells and tissues with underlying molecular networks provides a rational approach not only to characterizing the disease-relevant pathways, but also to identifying the network-based effective drug targets.

Increasing numbers of human disease-oriented omics data have been deposited in public databases, such as the Gene Expression Omnibus (GEO) repository (http://www.ncbi.nlm.nih.gov/geo) and the ArrayExpress archive (http://www.ebi.ac.uk/microarray-as/ae). Most of these are transcriptome datasets. Importantly, they really include the data that have potentially valuable information on molecular biomarkers and networks of the diseases, when they are reanalyzed by appropriate bioinformatics approaches, followed by validation of *in silico* observations with *in vitro* and *in vivo* experiments.[12]

The present review has focused on bioinformatics approaches to identifying MS-associated molecular biomarkers and networks from high-throughput data of omics studies.

Global gene expression analysis

DNA microarray technology is an innovative approach that allows us to systematically monitor the genome-wide gene expression pattern of disease-affected tissues and cells. This approach enables us to illustrate most efficiently a global picture of cellular activity by the messenger RNA (mRNA) expression levels as an indicator, although the levels of mRNA do not always correlate with the levels of proteins directly involved in cellular function. However, the use of DNA microarray is more convenient to collect temporal and spatial snapshots of gene expression than the conventional mass spectrometry, which is often hampered by limited resolution of protein separation. In transcriptome analysis, we could logically assume that a set of coregulated genes might have similar biological functions within the cells.

First of all, I would like to briefly overview the gene expression analysis (Fig. 1). In general, total RNA fractions containing mRNA species are extracted from cells and tissues, individually labeled with fluorescent dyes, and processed for hybridization with thousands of oligonucleotides of known sequences immobilized on the arrays. After washing, they are processed for signal acquisition on a scanner. Various types of microarrays are currently available, although the MicroArray Quality Control (MAQC) project verified that the core results are well reproducible among different platforms used.[13] However, it is recommended that each experiment should contain biological replicates to validate reproducibility of the observations. The raw data are normalized by representative methods, including the quantile normalization method and the Robust MultiChip Average (RMA) method using the R software of the Bioconductor package (cran.r-project.org) or the GeneSpring software (Agilent Technology, Palo Alto, CA, USA).

To identify differentially expressed genes (DEG) among distinct samples, the normalized data are processed for statistical analysis using *t*-test for comparison between two groups or analysis of variance (ANOVA) for comparison among more than three groups, followed by the multiple comparison test with the Bonferroni correction or by controlling false discovery rate (FDR) below 0.05 to adjust *P*-values.

In the next step, the levels of expression of DEG should be validated by quantitative reverse transcription polymerase chain reaction (qRT–PCR). The normalized data are also processed for hierarchical

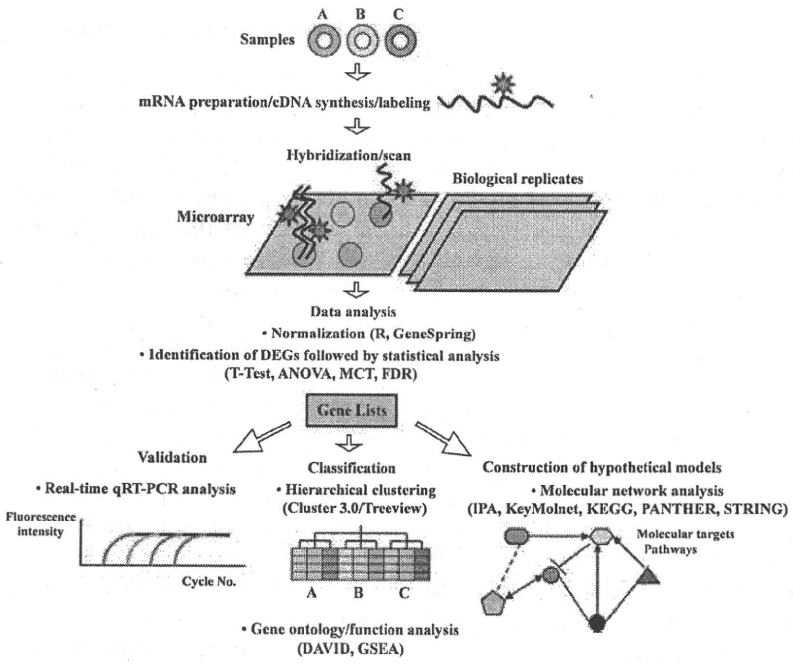

Figure 1 The load map from global gene expression profiling to molecular network analysis. Total RNA samples labeled with fluorescent dyes are processed for hybridization with oligonucleotide probes on the arrays, which should include biological replicates. They are processed for signal acquisition on a scanner. To identify the list of differentially expressed genes (DEG) among the samples, the normalized data are processed for statistical analysis, followed by validation by quantitative reverse transcription polymerase chain reaction (qRT-PCR). They are also processed for hierarchical clustering analysis and gene ontology and function analysis. To identify biologically relevant molecular pathways, the list of DEG is imported into pathway analysis tools endowed with a comprehensive knowledgebase. ANOVA, analysis of variance; DAVID, Database for Annotation, Visualization and Integrated Discovery; FDR, false discovery rate; GSEA, Gene Set Enrichment Analysis; IPA, Ingenuity Pathways Analysis; KEGG, Kyoto Encyclopedia of Genes and Genomes; MCT, multiple comparison test; PANTHER, Protein Analysis Through Evolutionary Relationships; and STRING; Search Tool for the Retrieval of Interacting Genes/Proteins.

clustering analysis to classify the expression of profile-based groups of genes and samples by using GeneSpring or the open-access resources, such as Cluster 3.0 (bonsai.ims.u-tokyo.ac.jp/~mdehoon/software/cluster) and TreeView (sourceforge.net/projects/jtreeview). The Gene ID Conversion tool of the Database for Annotation, Visualization and Integrated Discovery (DAVID) (david.abcc.ncifcrf.gov)[14] converts the large-scale array-specific probe IDs into the corresponding Entrez Gene IDs, HUGO Gene Symbols, Ensembel Gene IDs or UniProt IDs, being more convenient for application to the downstream analysis. Both the DAVID Functional annotation tool and the Gene Set Enrichment Analysis (GSEA) tool (www.broad.mit.edu/gsea/downloads.jsp)[15] are open-access resources that help us to identify a set of enriched genes with a specified functional annotation in the entire list of genes. Many other approaches for preprocessing microarray data are applicable, and the resources are available elsewhere.

Molecular network analysis

To identify biologically relevant molecular pathways from large-scale data, we could analyze them by using a battery of pathway analysis tools endowed with a comprehensive knowledgebase; that is, Kyoto Encyclopedia of Genes and Genomes (KEGG; http://www.kegg.jp), the Protein Analysis Through Evolutionary Relationships (PANTHER) classification system (http://www.pantherdb.org), Search Tool for the Retrieval of Interacting Genes/Proteins (STRING; string.embl.de), Ingenuity Pathways Analysis (IPA; Ingenuity Systems, http://www.ingenuity.com) and KeyMolnet (Institute of Medicinal Molecular Design, http://www.immd.co.jp) (Fig. 1). KEGG, PANTHER and STRING are open-access databases, whereas IPA and KeyMolnet are commercial databases updated regularly. Both transcriptome and proteome data are acceptable for all the databases described here.

KEGG systematically integrates genomic and chemical information to create the whole biological

system *in silico*.[16] KEGG includes manually curated reference pathways that cover a wide range of metabolic, genetic, environmental and cellular processes, and human diseases. Currently, KEGG contains 108 983 pathways generated from 358 reference pathways. PANTHER, operating on the computational algorithms that relate the evolution of protein sequences to the evolution of protein functions and biological roles, provides a structured representation of protein function in the context of biological reaction networks.[17] PANTHER includes the information on 165 regulatory and metabolic pathways, manually curated by expert biologists. By uploading the list of Gene IDs, the PANTHER gene expression data analysis tool identifies the genes in terms of over- or under-representation in canonical pathways, followed by statistical evaluation by multiple comparison test with the Bonferroni correction. STRING is a database that contains physiological and functional protein-protein interactions composed of 2 590 259 proteins from 630 organisms.[18] STRING integrates the information from numerous sources, including experimental repositories, computational prediction methods and public text collections. By uploading the list of UniProt IDs, STRING illustrates the union of all possible association networks.

IPA is a knowledgebase that contains approximately 2 270 000 biological and chemical interactions and functional annotations with definite scientific evidence, curated by expert biologists.[19] By uploading the list of Gene IDs and expression values, the network-generation algorithm identifies focused genes integrated in a global molecular network. IPA calculates the score *P*-value, the statistical significance of association between the genes and the networks by the Fisher's exact test.

KeyMolnet contains knowledge-based content on 123 000 relationships among human genes and proteins, small molecules, diseases, pathways and drugs, curated by expert biologists.[20] They are categorized into the core content collected from selected review articles with the highest reliability or the secondary contents extracted from abstracts of PubMed and Human Reference Protein database (HPRD). By importing the list of Gene ID and expression values, KeyMolnet automatically provides corresponding molecules as a node on networks. The "common upstream" network-search algorithm enables us to extract the most relevant molecular network composed of the genes coordinately regulated by putative common upstream transcription factors. The "neighboring" network-search algorithm selected one or more molecules as starting points to generate the network of all kinds of molecular interactions around starting molecules, including direct activation/inactivation, transcriptional activation/repression, and the complex formation within the designated number of paths from starting points. The "N-points to N-points" network-search algorithm identifies the molecular network constructed by the shortest route connecting the start-point molecules and the end-point molecules. The generated network was compared side-by-side with 430 human canonical pathways of the KeyMolnet library. The algorithm counting the number of overlapping molecular relations between the extracted network and the canonical pathway makes it possible to identify the canonical pathway showing the most significant contribution to the extracted network. The significance in the similarity between both is scored following the formula, where O is the number of overlapping molecular relations between the extracted network and the canonical pathway, V is the number of molecular relations located in the extracted network, C is the number of molecular relations located in the canonical pathway, T is the number of total molecular relations, and X is the sigma variable that defines coincidence.

$$\text{Score} = -\log_2(\text{Score}[P])$$

$$\text{Score}(P) = \sum_{x=O}^{\text{Min}(C,V)} f(x)$$

$$f(x) = {}_C C_x \cdot {}_{T-C} C_{V-x} / {}_T C_V$$

Biomarkers for predicting MS relapse

Molecular mechanisms underlying acute relapse of MS remain currently unknown. If molecular biomarkers for MS relapse are identified, we could predict the timing of relapses, being invaluable to start the earliest preventive intervention.

By gene expression profiling with Affymetrix Human Genome U133 plus 2.0 arrays, Corvol et al. identified 975 genes that separate clinically isolated syndrome (CIS) into four groups.[21] Surprisingly, 92% of patients in group 1 were characterized by a subset of 108 genes converted to clinically definite MS (CDMS) within 9 months of the first attack. They suggest downregulation of TOB1, a negative regulator of T cell proliferation as a marker predicting the conversion from CIS to CDMS.

By gene expression profiling with Affymetrix Human Genome U133A2 arrays, Achiron et al. showed that 1578 DEG of peripheral blood mononuclear cells (PBMC) of RRMS patients, differentiating

acute relapse from remission, are enriched in the apoptosis-related pathway, in which proapoptotic genes are downregulated, whereas antiapoptotic genes are upregulated during acute relapse.[22] The same group also compared 62 patients with CDMS and 32 patients with CIS by combining gene expression profiling with the support vector machine (SVM)-based prediction of time to the next acute relapse, setting a two stage predictor composed of First Level Predictors (FLP) and Fine Turning Predictors (FTP).[23] They identified three sets of the best 10-gene FLP that predict the next relapse with a resolution of 500 days and four sets of the best 9-gene FTP that predict the forthcoming relapse with a resolution of 50 days. The predictor genes are enriched in the TGFB2-related signaling pathway. More recently, Achiron et al. compared nine subjects who developed MS during a 9-year follow-up period (the preactive stage of MS; MS-to-be) and 11 control subjects unaffected with MS (MS-free) by gene expression profiling.[24] They found downregulation of nuclear receptor NR4A1 in the preactive stage of MS, suggesting that self-reactive T cells are not eliminated in the MS-to-be population, owing to a defect in the NR4A1-dependent apoptotic mechanism.

By gene expression profiling with a custom microarray of the Peter MacCallum Cancer Institute, Arthur et al. showed that a set of dysregulated genes in peripheral blood cells during the relapse and the remission phases of RRMS are enriched in the categories involved in apoptosis and inflammation, when annotated according to the GOstat program.[25] They also found upregulation of TGFB1 during the relapse. These observations support the working hypothesis that MS relapse involves an imbalance between promoting and preventing apoptosis of autoreactive and regulatory T cells. By gene expression analysis with Affymetrix Human Genome U133 plus 2.0 arrays, Brynedal et al. showed that MS relapses reflect the gene expression change in PBMC, but not in cerebrospinal fluid (CSF) lymphocytes, suggesting the importance of initial events triggering relapses occurring outside the CNS.[26]

By gene expression profiling with a custom DNA microarray (Hitachi Life Science, Saitama, Japan), we identified 43 DEG in peripheral blood $CD3^+$ T cells between the peak of acute relapse and the complete remission of RRMS patients.[27] We isolated highly purified $CD3^+$ T cells, because autoreactive pathogenic and regulatory cells, which potentially play a major role in MS relapse and remission, might be enriched in this fraction. By using 43 DEG as a set of discriminators, hierarchical clustering separated the cluster of relapse from that of remission. The molecular network of 43 DEG extracted by the common upstream search of KeyMolnet showed the most significant relationship with transcriptional regulation by the nuclear factor-kappa B (NF-κB). NF-κB is a central regulator of innate and adaptive immune responses, cell proliferation, and apoptosis.[28] A considerable number of NF-κB target genes activate NF-κB itself, providing a positive regulatory loop that amplifies and perpetuates inflammatory responses, leading to persistent activation of autoreactive T cells in MS. These observations support the logical hypothesis that NF-κB plays a central role in triggering molecular events in T cells responsible for induction of acute relapse of MS, and suggest that aberrant gene regulation by NF-κB on T-cell transcriptome serves as a molecular biomarker for monitoring the clinical disease activity of MS. Supporting this hypothesis, increasing evidence has shown that NF-κB represents a central molecular target for MS therapy.[29]

We also studied the gene expression profile of purified $CD3^+$ T cells isolated from four Hungarian monozygotic MS twin pairs with a custom DNA microarray (Hitachi Life Science, Saitama, Japan).[30] By comparing three concordant pairs and one discordant pair, we identified 20 DEG aberrantly regulated between the MS patient and the genetically identical healthy subject. The molecular network of 20 DEG extracted by the common upstream search of KeyMolnet showed the most significant relationship with transcriptional regulation by the Ets transcription factor family. Ets transcription factor proteins, by interacting with various co-regulatory factors, control the expression of a wide range of target genes essential for cell proliferation, differentiation, transformation and apoptosis. Importantly, Ets-1, the prototype of the Ets family members, acts as a negative regulator of Th17 cell differentiation.[31] It is worthy to note that discordant monozygotic MS twin siblings do not show any genetic or epigenetic differences, as validated by whole genome sequencing analysis and genome-scale DNA methylation profiling.[8]

Biomarkers for predicting IFNβ responders

Although recombinant IFNβ therapy is widely used as the gold standard to reduce disease activity of MS, up to 50% of the patients continue to have relapses, followed by progression of disability. If molecular biomarkers for IFNβ responsiveness are identified, we could use the best treatment options depending on the patients, being invaluable to establish the personalized therapy of MS.

By genome-wide screening of single-nucleotide polymorphisms (SNP) with Affymetrix Human 100K SNP arrays, Byun et al. identified allelic differences between IFNβ responders and non-responders of RRMS patients in several genes, including HAPLN1, GPC5, COL25A1, CAST and NPAS3, although odds ratios of SNP differences of individual genes are fairly low.[32]

By gene expression profiling with Affymetrix Human Genome U133A Plus 2.0 arrays, Comabella et al. showed that IFNβ non-responders of RRMS patients after treatment for 2 years are characterized by the overexpression of type I IFN-induced genes in PBMC, associated with increased endogenous production of type I IFN by monocytes at pretreatment.[33] These observations suggest that a preactivated type I IFN signaling pathway is attributable to IFNβ non-responsiveness in MS. By gene expression profiling with Affymetrix Human Genome Focus arrays, Sellebjerg et al. showed that *in vivo* injection of IFNβ rapidly induces elevation of IFI27, CCL2 and CXCL10 in PBMC of MS patients, even after 6 months of treatment,[34] consistent with previous studies.[35] The induction of IFN-responsive genes is greatly reduced in patients with neutralizing antibodies (NAbs) against IFNβ.[34] In contrast, there exist no global differences in gene expression profiles of PBMC of RRMS patients between NAbs-negative IFNβ non-responders and responders.[36]

By gene expression profiling with Affymetrix Human Genome U133A/B arrays, Goertsches et al. found that IFNβ administration *in vivo* elevates a panel of IFN-responsive genes in PBMC of RRMS patients during a 2-year treatment, but it also downregulates several genes, including CD20, a known target of B-cell depletion therapy in MS.[37] By using the PATHWAY ARCHITECT software (Stratagene, La Jolla, CA, USA), they identified two major gene networks where upregulation of STAT1 and downregulation of ITGA2B act as a central molecule, although they did not further characterize the responder/non-responder-linked gene expression profiles.

By gene expression profiling with a custom array of the National Institutes of Health (NIH)/National Institute of Neurological Disorders and Stroke (NINDS) Microarray Consortium, Fernald et al. showed that a 1-week IFNβ administration *in vivo* induces a set of coregulated genes whose networks are related to immune- and apoptosis-regulatory functions, involving JAK-STAT and NF-κB cascades, whereas the networks of untreated subjects are composed of the genes of cellular housekeeping functions.[38] By combining kinetic RT–PCR analysis of expression of 70 genes in PBMC of RRMS with the integrated Bayesian inference system approach, the same group previously reported that nine sets of gene triplets detected at pretreatment, including a panel of caspases, well predict the response to IFNβ with up to 86% accuracy.[39]

By gene expression profiling with a custom microarary (Hitachi), we previously identified a set of interferon-responsive genes expressed in purified peripheral blood $CD3^+$ T cells of RRMS patients receiving IFNβ treatment.[40] IFNβ immediately induces a burst of expression of chemokine genes with potential relevance to IFNβ-related early adverse effects in MS.[41] The majority of the top 30 most significant DEG in $CD3^+$ T cells between untreated MS patients and healthy subjects are categorized into apoptosis signaling regulators.[42] Furthermore, we found that T cell gene expression profiling classifies a heterogeneous population of Japanese MS patients into four distinct subgroups that differ in the disease activity and therapeutic response to IFNβ.[43] We identified 286 DEG expressed between 72 untreated Japanese MS patients and 22 age- and sex-matched healthy subjects. By importing the list of 286 DEG into the common upstream search of KeyMolnet, the generated network showed the most significant relationship with transcriptional regulation by NF-κB.[30] Although none of the single genes alone serve as a MS-specific biomarker gene, NR4A2 (NURR1), a target of NF-κB acting as a positive regulator of IL-17 and IFNγ production, is highly upregulated in MS T cells.[42,43] It is worthy to note that IFNβ is beneficial in the disease induced by Th1 cells, but detrimental in the disease mediated by Th17 cells in mouse experimental autoimmune encephalomyelitis (EAE), and IFNβ non-responders in RRMS patients show higher serum IL-17F levels, suggesting that IL-17 serves as a biomarker predicting a poor IFNβ response in MS.[44]

Molecular networks of MS brain lesion proteome

Recently, Han et al. investigated a comprehensive proteome of six frozen MS brains.[7] Proteins were prepared from small pieces of brain tissues isolated by laser-captured microdissection (LCM), and they were characterized separately by the standard histological examination, and classified into acute plaques (AP), chronic active plaques (CAP) or chronic plaques (CP) based on the disease activity. The proteins were then separated on one-dimensional SDS-PADE gels, digested in-gel with trypsin, and peptide fragments were processed for mass spectrometric